

Constraints on the generalized natural inflation after Planck 2018

Nan Zhang¹, Ya-Bo Wu¹, Jun-Wang Lu², Chu-Wen Sun¹, Li-Jie Shou¹, Hai-Zhou Xu¹

¹ Department of Physics, Liaoning Normal University, Dalian 116029, P.R.China

² School of Physics and Electronics, Qiannan Normal University for Nationalities, Duyun 558000, P.R.China

E-mail: ybwu61@163.com

Abstract. Based on the dynamics of single scalar field slow-roll inflation and the theory of reheating, we investigate the generalized natural inflationary (GNI) model. Concretely, we give constraints on the scalar spectral index n_s and tensor-to-scalar ratio r for Λ CDM + r model according to the latest data from Planck 2018 TT,TE,EE+lowE+lensing (P18) and BICEP2/Keck 2015 season (BK15), i.e., $n_s = 0.9659 \pm 0.0044$ at 68% confidence level (CL) and $r < 0.0623$ at 95%CL. We find that the GNI model is favored by P18 plus BK15 in the ranges of $\log_{10}(f/M_p) = 0.62^{+0.17}_{-0.18}$ and $m = 0.35^{+0.13}_{-0.23}$ at 68%CL. In addition, the corresponding predictions of the general and two-phase reheating are respectively discussed. It follows that the parameter m has the significant effect on the model behaviors.

1. Introduction

Inflation is a widely accepted supplement to the successful standard big bang theory. The existence of inflation phase can lead to a rapid accelerated expansion period of the universe in order to solve the problems such as the flatness, the horizon, etc [1, 2, 3, 4, 5]. It can also give a superior interpretation of the origin of structure and cosmic microwave background (CMB) [6, 7, 8]. Then the cold and empty universe during inflation is heated through the reheating phase, the radiation particles corresponding to the standard model are also generated in the reheating epoch. In order to investigate the properties of inflation period, many kinds of models have been proposed, such as the R^2 model [9], hilltop model [10], natural inflation model [11, 12], α attractors [13, 14] and so on. Most models are slow-roll ones taking a scalar field as the inflaton and making it slowly roll toward its true ground state [15, 16, 17].

As we know, the natural inflationary (NI) model is a kind of single field slow-roll inflationary models. It was proposed in Refs. [11] with the potential form $V(\phi) = \Lambda^4[1 \pm \cos(N\phi/f)]$, in which the choice of sign has no effect on the results, and usually, taking $N = 1$. The model parameter f is called the decay constant [18]

and $f \gtrsim 0.3M_p$ [12]. The NI model is widely studied in many literatures because of its simple potential form and theoretically well motivation [19, 20, 21]. However, from the aspect of recent observation, the NI model is disfavored by the data from Planck 2018 [22, 23, 24, 25, 26, 27] and BICEP2/Keck with inclusion of 95 GHz band (BK14) [28].

The “generalized” version of the NI model was proposed in Ref. [18], which adds the model parameter m on the basis of the NI model, i.e., $V(\phi) = 2^{1-m}\Lambda^4[1 + \cos(\frac{\phi}{f})]^m$ [18]. Here, we call it the generalized natural inflationary (GNI) model. Evidently, the NI model is a special case of the GNI model corresponding to $m = 1$. Moreover, for the investigation of the GNI model in Ref. [18], the authors discussed only the proper ranges of values of N_* by using the tight constraint of $0 \lesssim w_{re} \lesssim 0.25$ [29] and taking $m = 1$ in the most cases. Whereas the corresponding results to the cases of $m \neq 1$ have been rarely discussed. Thus, it is an interesting issue that how the parameter m influences the behaviors of the GNI model. In addition, we are inspired to wonder if the GNI model, which is the broad class of the NI model, could be favored by the recent data from Plack 2018 TT,TE,EE+lowE+lensing (P18) and BICEP2/Keck 2015 season (BK15) [30] due to the existence of parameter m . These are just our motivations and purposes of investigating the GNI model in this paper.

Based on the above, this paper will focus on the key parameters for the inflationary models, i.e., scalar spectral index n_s , tensor-to-scalar ratio r , the e-folding number N_* , the reheating e-folding number N_{re} , the reheating temperature T_{re} and the effective average equation of state (EoS) w_{re} [31, 32, 33], etc. Specifically, we will investigate the constraints on n_s and r by means of the public codes Cosmomic [34] according to the data from P18 plus BK15, as well as the allowable parameter space of the GNI model, in which we will calculate the running spectral index α_s . In addition, we will study two different mechanisms of the reheating phase, one is the general reheating phase, and the other is a two-phase reheating process [35, 36]. Our research results indicate that the GNI model is favored by P18 plus BK15 in the ranges of $\log_{10}(f/M_p) = 0.62^{+0.17}_{-0.18}$ and $m = 0.35^{+0.13}_{-0.23}$ at 68%CL. Moreover, the parameter m has the significant effect on the model behaviors. The evolutions of the reheating parameters of the GNI model are also discussed in detail, including N_{re} , T_{re} in the general reheating phase and the oscillation e-folding number N_{sc} , temperature $T_{re}e^{N_{th}}$, coupling constant g in the two-phase reheating.

This paper is organized as follows. In Sec. 2, we briefly review the depiction of single scalar field slow-roll inflation, the constraints on n_s and r from the data of P18 plus BK15 are obtained. In Sec. 3, we investigate the validity of the GNI model, i.e., the constraints on the model parameters according to the observational data. Then in Sec. 4, we discuss the general reheating phase and the two-phase reheating of the GNI model. Sec. 5 presents the conclusions.

2. The single field slow-roll inflation

We will give a brief review of a single field inflationary model [19, 20, 23, 25, 27, 36, 37, 38] and we start with the equations of motion induced by a scalar field ϕ in the frame of spatially flat FRW background universe,

$$H^2 = \frac{1}{3M_p^2} \left(\frac{1}{2} \dot{\phi}^2 + V(\phi) \right), \quad (1)$$

$$\ddot{\phi} + 3H\dot{\phi} = -V'(\phi), \quad (2)$$

where $H \equiv \dot{a}/a$ is the Hubble parameter, $V(\phi)$ is the potential of field ϕ , $M_p \equiv \frac{1}{\sqrt{8\pi G}} \simeq 2.435 \times 10^{18}$ GeV is the reduced Planck mass, the dot denotes differentiation with respect to cosmic time t and the prime denotes differentiation with respect to ϕ .

In the case of slow-roll inflation, the potential term dominates the total energy density and the scalar field changes slowly with time, Eqs. (1) and (2) can be written as follows:

$$H^2 \simeq \frac{V(\phi)}{3M_p^2}, \quad (3)$$

$$3H\dot{\phi} \simeq -V'(\phi). \quad (4)$$

Thus, the parameter N_* , which represents the e-folding number between the pivot scale k_* exiting from the Hubble radius and the end of inflation, can be expressed in terms of the potential $V(\phi)$ under the slow-roll approximation

$$N_* \equiv \ln \frac{a_{end}}{a_*} = \int_{t_*}^{t_{end}} H dt \simeq -\frac{1}{M_p^2} \int_{\phi_*}^{\phi_{end}} \frac{V(\phi)}{V'(\phi)} d\phi, \quad (5)$$

where the subscripts “*” and “end” correspond to crossing the horizon and the end of inflation, respectively.

Next, introducing the slow-roll parameters:

$$\epsilon_v = \frac{M_p^2}{2} \frac{V'(\phi)^2}{V(\phi)^2}, \quad (6)$$

$$\eta_v = M_p^2 \frac{V''(\phi)}{V(\phi)}, \quad (7)$$

The power spectra of curvature and tensor perturbations $\mathcal{P}_{\mathcal{R}}$, \mathcal{P}_t can be well approximated in the case of the usual single field slow-roll inflationary models, thus the scalar spectral index n_s and the tensor spectral index n_t can be expressed as:

$$n_s \simeq 1 - 6\epsilon_v + 2\eta_v, \quad (8)$$

$$n_t \simeq -2\epsilon_v. \quad (9)$$

Then making use of the scalar power spectra amplitude $A_s \simeq \frac{V}{24\pi^2 M_p^4 \epsilon_v}$ and the tensor amplitude $A_t \simeq \frac{2V}{3\pi^2 M_p^4}$, the tensor-to-scalar ratio r can be obtained as

$$r = \frac{A_t}{A_s} \simeq 16\epsilon_v, \quad (10)$$

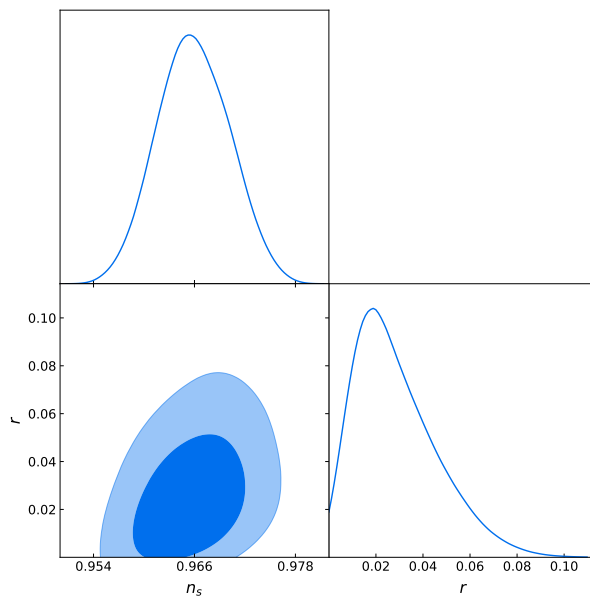


Figure 1. The marginalized contour plots and likelihood distributions for n_s and r at 68%CL and 95%CL from the data of P18+BK15, respectively.

which means n_t is not a free parameter due to $r \simeq -8n_t$.

In this paper, we adopt the data from P18 [27] plus BK15 [30] to obtain the constraints on n_s and r for Λ CDM + r model, they are given as follows by means of the available Cosmomic code [34]:

$$n_s = 0.9659 \pm 0.0044 \quad (68\%CL), \quad (11)$$

$$r < 0.0623 \quad (95\%CL). \quad (12)$$

The contour plots for n_s and r are shown in Figure 1. It indicates that the power spectrum of curvature perturbation deviates from the exact scale-invariant power spectrum at more than 7σ CL.

3. The constraints on the model parameters of the GNI model

As we know, the ordinary NI potential was simply generalized by adding one parameter m in Ref. [18], here we call this model as the generalized natural inflationary (GNI) model. The form of potential for the GNI model is expressed as follows:

$$V(\phi) = 2^{1-m} \Lambda^4 \left[1 + \cos\left(\frac{\phi}{f}\right) \right]^m, \quad (13)$$

where the energy density Λ^4 , decay constant f and the constant m are the parameters of the model. It follows that when $m = 1$, it can reduce to the so-called NI model. If $f \rightarrow \infty$, the NI model seems to behave like the chaotic inflationary model. Similarly, the GNI model behaves as a pure power law model when $f \rightarrow \infty$ [18]. Figure 2 shows the evolving tendency of the potential roughly. The horizontal axis is ϕ/M_p , the vertical

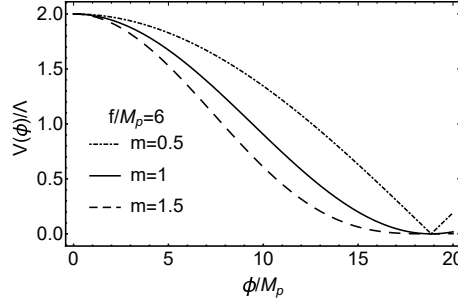


Figure 2. The evolving trajectories of $V(\phi)$ in the GNI model for $m = 0.5, 1$ and 1.5 , respectively. Here, $f/M_p = 6$ is taken.

axis is $V(\phi)/\Lambda^4$. From the trajectories, we can find that if f is a fixed value, such as $f/M_p = 6$, $V(\phi)$ changes more slowly for smaller m in the beginning and becomes steep in the end, the trajectories reach zero at the same value of ϕ .

According to Eqs. (6) and (7), the slow-roll parameters ϵ_v and η_v of the GNI model can be given as follows:

$$\epsilon_v = \frac{M_p^2 m^2}{2f^2} \left[\frac{1 - \cos(\phi/f)}{1 + \cos(\phi/f)} \right], \quad (14)$$

$$\eta_v = -\frac{M_p^2}{f^2} \left[\frac{m - m^2(1 - \cos(\phi/f))}{1 + \cos(\phi/f)} \right]. \quad (15)$$

Thus, n_s and r can be expressed as:

$$n_s = 1 - \frac{M_p^2}{f^2} \left[\frac{m^2(1 - \cos(\phi/f) + 2m)}{1 + \cos(\phi/f)} \right], \quad (16)$$

$$r = \frac{8M_p^2 m^2}{f^2} \left[\frac{1 - \cos(\phi/f)}{1 + \cos(\phi/f)} \right]. \quad (17)$$

And the e-folding number N_* is derived as:

$$N_* = \frac{f^2}{mM_p^2} \ln \frac{1 - \cos(\phi_{end}/f)}{1 - \cos(\phi_*/f)}. \quad (18)$$

When $\epsilon_v = \epsilon_{end} = 1$, ϕ_{end} can be obtained from Eq. (14) as follows

$$\phi_{end} = f \arccos \frac{m^2 M_p^2 - 2f^2}{m^2 M_p^2 + 2f^2}. \quad (19)$$

Substituting Eq. (19) into Eq. (18), ϕ_* can be derived as

$$\phi_* = f \arccos \left[1 - \frac{4f^2}{m^2 M_p^2 + 2f^2} \exp\left(-\frac{mM_p^2}{f^2} N_*\right) \right]. \quad (20)$$

It follows that ϕ_* is the function of (N_*, f, m) . In this case, Eqs. (16) and (17) become into

$$n_s = 1 - \frac{mM_p^2}{f^2} \left[1 + \frac{2f^2(m+1) \exp\left(-\frac{mM_p^2}{f^2} N_*\right)}{m^2 M_p^2 + 2f^2(1 - \exp\left(-\frac{mM_p^2}{f^2} N_*\right))} \right], \quad (21)$$

$$r = \frac{16m^2M_p^2 \exp(-\frac{mM_p^2}{f^2}N_*)}{m^2M_p^2 + 2f^2(1 - \exp(-\frac{mM_p^2}{f^2}N_*))}. \quad (22)$$

It is easy to see that when taking $m = 1$, Eqs. (21) and (22) can reduce to the results in the NI model. Hence, the predictions of n_s and r in the GNI model are given in Figure 3, N_* is taken in the usual range of $[50, 60]$, and the shaded regions represent the constraints given by P18+BK15 at 68% and 95% CL, respectively. It can be found

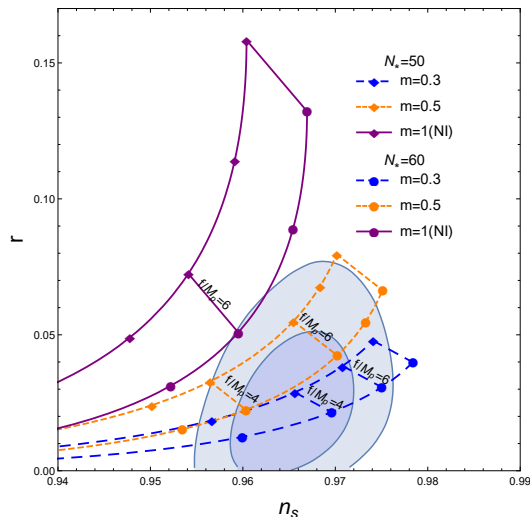


Figure 3. The plots of r and n_s in the GNI model for $m = 0.3, 0.5$ and 1 , respectively. $N_* \in [50, 60]$ is taken and the shaded regions represent the constraints given by P18+BK15 at 68% and 95% CL, respectively.

that the case of $m = 1$ (NI model) is disfavored by the data of P18 plus BK15, however, the case of $m < 1$ can provide the small values of r in the proper ranges of values of n_s . Thus, the GNI model is worth investigating in the case of $m < 1$.

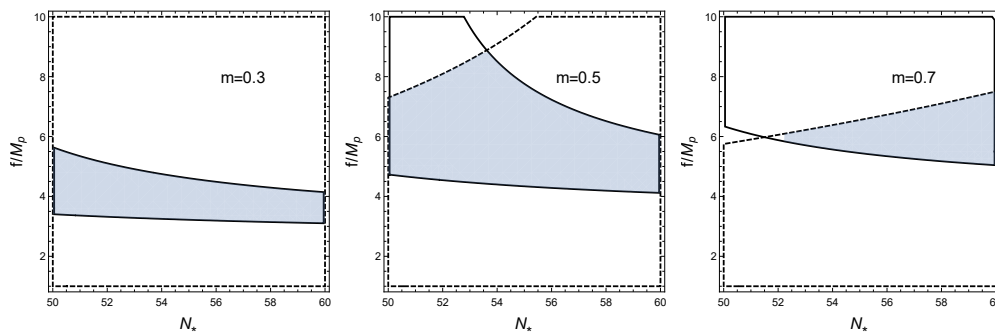


Figure 4. Allowed ranges of values of N_* and f for $m = 0.3, 0.5$ and 0.7 , respectively. In each panel, the solid curves bracket the range of values of $n_s = 0.9659 \pm 0.0044$, the dotted curves bracket the range of values of $r < 0.0623$.

Figure 4 shows the allowed ranges of values of N_* and f when taking $m = 0.3, 0.5$ and 0.7 , respectively. It can be seen that the allowable parameter space firstly becomes

large and then becomes small with increasing m according to the areas of the shaded regions in Figure 4. Moreover, when $m = 0.7$, $N_*^{min} = 51.1$ can be obtained, which suggests that the minimum value of N_* could be larger than 50 if the value of m is relatively large enough. Besides, the value of f/M_p is smaller than 10 from Figure 4.

Below, N_* , f/M_p and m are all taken as free parameters of the GNI model, the contour plots by means of the public code Cosmomc are shown in Figure 5. It shows

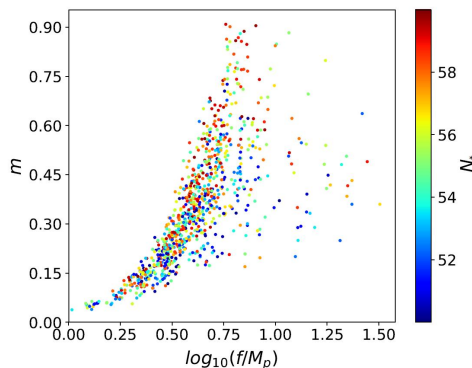


Figure 5. The contour plots for N_* , f/M_p and m in the GNI model from the data of P18+BK15, the values of N_* are represented by the color of the points.

that the majority of the points locate in the range of $f/M_p < 10$, and the points corresponding to the small values of N_* vanish when the value of m is slightly big. This result is consistent with our simple predictions in Figure 4. In order to provide a direct sketch, we give the marginalized contour plots for f/M_p and m in the usual range $N_* \in [50, 60]$ in Figure 6. The constraints on f/M_p and m at 68%CL can be read as

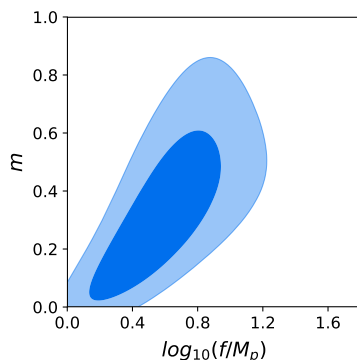


Figure 6. The marginalized contour plots for f/M_p and m in the GNI model at 68%CL and 95%CL from the data of P18+BK15, respectively.

$$\log_{10}(f/M_p) = 0.62^{+0.17}_{-0.18}, \quad (23)$$

$$m = 0.35^{+0.13}_{-0.23}. \quad (24)$$

Moreover, we can also calculate the higher-order slow-roll parameter $\xi_v^2 = M_p^4 \frac{V'(\phi)V'''(\phi)}{V(\phi)^2}$ and the running of the scalar spectral index $\alpha_s \equiv \frac{dn_s}{d \ln k} \simeq 16\epsilon_v \eta_v - 24\epsilon_v^2 - 2\xi_v^2$ of the GNI model as follows:

$$\xi_v^2 = m^2 M_p^4 \frac{4f^2 m^2 - (3m-1)(2f^2 + m^2 M_p^2) e^{\frac{m M_p^2}{f^2} N_*}}{(-2f^3 + (2f^3 + f m^2 M_p^2) e^{\frac{m M_p^2}{f^2} N_*})^2}, \quad (25)$$

$$\alpha_s \simeq \frac{-2m^2(m+1)M_p^4(2f^2 + m^2 M_p^2) e^{\frac{m M_p^2}{f^2} N_*}}{(-2f^3 + (2f^2 + m^2 M_p^2) f e^{\frac{m M_p^2}{f^2} N_*})^2}. \quad (26)$$

In Figure 7, we plot α_s with respect to N_* , the values of f/M_p and m are taken as the boundary values of Eqs. (23)(24). It shows that the value of α_s is negative and its value increases with increasing N_* for the fixed values of f and m . And the allowable range of values of α_s becomes wide with increasing m when $\log_{10}(f/M_p) = 0.62_{-0.18}^{+0.17}$, $-0.0006 \lesssim \alpha_s \lesssim -0.0001$ can be found from Figure 7.

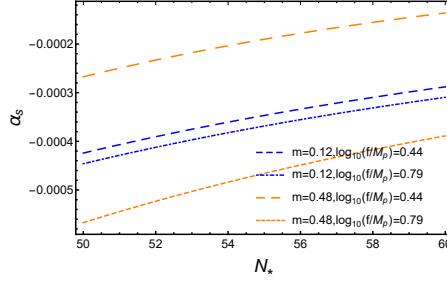


Figure 7. The running of the scalar spectral index α_s with respect to N_* , the values of f/M_p and m are taken as the boundary values of the GNI model given by the data from P18+BK15 at 68% CL.

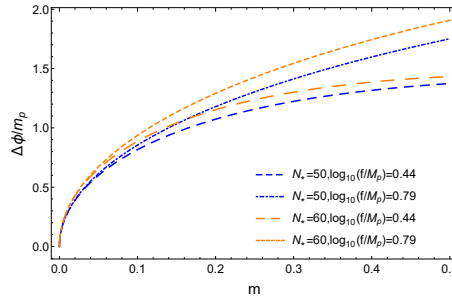


Figure 8. The excursion $\Delta\phi/m_p$ with respect to m , the values of N_* are taken as 50, 60, and the values of f are taken as the boundary values of the GNI model given by the data from P18+BK15 at 68% CL, respectively.

In addition, another important issue of single field inflationary model is the so-called trans-Planckian field excursion of the inflaton. This problem appears in the model with large tensor-to-scalar ratio r , as indicated by the Lyth bound [39], and will spoil the

basis of the effective field theory. In the GNI model considered here, r is constrained to be small, so this will not be a serious problem. We plot the excursion $\Delta\phi = |\phi_* - \phi_{end}|$ of the inflaton with respect to m in Figure 8, and find that the excursion $\Delta\phi$ decreases with lower m and f . One can see from Figure 8 that with small f and m , which fit the observational data, $\Delta\phi$ might be below the Planck mass $m_p = 1/\sqrt{G} = 1.2 \times 10^{19} \text{ GeV}$.

4. The reheating phase of the GNI model

Following the approaches proposed in Refs. [36, 40, 41], as for the reheating phase, the starting point is the relation $k = aH$. It leads to:

$$\begin{aligned} 0 &= \ln \frac{a_{end}}{a_*} + \ln \frac{a_{re}}{a_{end}} + \ln \frac{a_0}{a_{re}} + \ln \frac{k_*}{a_0 H_*} \\ &= N_* + N_{re} + \ln \frac{a_0}{a_{re}} + \ln \frac{k_*}{a_0 H_*}, \end{aligned} \quad (27)$$

where the subscript “ re ” corresponds to the end of reheating, a_0 means the present value of scale factor which is equal to 1, the pivot scale k_* is chosen to be 0.05 Mpc^{-1} . Based on the conservation of entropy density $g_{re} a_{re}^3 T_{re}^3 = g_\gamma a_0^3 T_\gamma^3 + \frac{7}{8} g_\nu a_0^3 T_\nu^3$ and the relationship of temperature $T_\nu/T_\gamma = (4/11)^{1/3}$, the expression of a_{re}/a_0 can be written as $a_{re}/a_0 = (43/11g_{re})^{1/3}/(T_\gamma/T_{re})$, $T_\gamma = 2.7255 \text{ K}$ is a known quantity. The parameter g with subscripts is the effect number of degrees of freedom, $g_\gamma = 2$ and $g_\nu = 6$, g_{re} is assuming as 10^3 for single scalar field inflationary models in keeping with Planck results [25, 27, 42].

Considering the energy density of the universe at the end of the reheating $\rho_{re} = g_{re} \frac{\pi^2}{30} T_{re}^4$ and the continuity equation $\rho_{re} = \rho_{end} \exp[-3(1 + w_{re})N_{re}]$, the expression of temperature at the end of reheating can be obtained,

$$T_{re} = \exp\left[-\frac{3}{4}(1 + w_{re})N_{re}\right] \left(\frac{45V_{end}}{g_{re}\pi^2}\right)^{1/4}, \quad (28)$$

where w_{re} is regarded as the average EoS during reheating, V_{end} is used to substitute for ρ_{end} [42]. The relation between V_{end} and ρ_{end} can be deduced by taking $\epsilon_H = \frac{3}{2}(1 + w) = \epsilon_{end}$, and $\epsilon_{end} = 1$ is the sign of the end of inflation. $\epsilon_H \equiv -\dot{H}/H^2$ is the first Hubble hierarchy parameter, in slow-roll approximation, $\epsilon_H \simeq \epsilon_v$. For a scalar field, $w \equiv P/\rho = \frac{\frac{1}{2}\dot{\phi}^2 - V}{\frac{1}{2}\dot{\phi}^2 + V}$. After a simple calculation, we can get $\rho_{end} \simeq \frac{3}{2}V_{end}$. Hence, the third term on the righthand in Eq. (27) can be rewritten as $\ln \frac{a_0}{a_{re}} = \frac{1}{3} \ln \frac{11g_{re}}{43} - \frac{3}{4}(1 + w_{re})N_{re} + \frac{1}{4} \ln \frac{45V_{end}}{g_{re}\pi^2} - \ln T_\gamma$. Therefore, H_* is the only uncertain quantity in Eq. (27) and it can be fixed by combining Eqs. (3)(10) with the scalar amplitude A_s as $A_s \simeq H_*^2/(\pi^2 M_p^2 r/2)$.

Finally, the expression of the e-folding number N_{re} during reheating can be written as follows:

$$\begin{aligned} N_{re} &= \frac{4}{1 - 3w_{re}} \left[-N_* - \frac{1}{3} \ln \frac{11g_{re}}{43} - \frac{1}{4} \ln \frac{45V_{end}}{g_{re}\pi^2} \right. \\ &\quad \left. - \ln \frac{k_*}{T_\gamma} + \frac{1}{2} \ln(\pi^2 M_p^2 (r/2) A_s) \right]. \end{aligned} \quad (29)$$

4.1. The general reheating phase

For general reheating epoch, substituting the expressions of V_{end} and r into Eqs. (28) and (29), N_{re} and T_{re} can be obtained for the GNI model. As we know, the EoS for the scalar field is in the range of $[-1, 1]$, and it should be smaller than $-1/3$ to meet the requirement of accelerating expansion. Thus, when discussing the reheating phase, the value of w_{re} is usually taken in the range of $-1/3 \leq w_{re} \leq 1$. In addition, it is easy to find the denominator of Eq. (29) will vanish if $w_{re} = 1/3$, which means $w_{re} = 1/3$ is the boundary of different evolution of tendencies for reheating parameters. The evolving trajectories of the reheating e-folding number N_{re} and the reheating temperature T_{re} are illustrated in Figure 9, three different values of w_{re} are considered in each panel as $w_{re} = -1/3, 0$ and 1 . The values of f/M_p and m are taken as the boundary values of Eqs. (23) and (24).

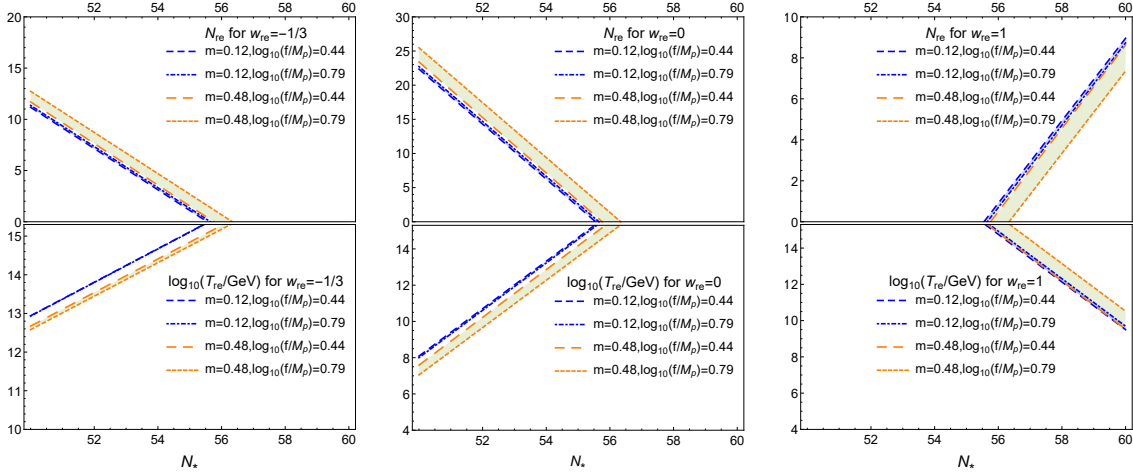


Figure 9. The evolving trajectories of the reheating e-folding number N_{re} and the reheating temperature T_{re}/GeV with respect to N_* are respectively plotted in the upper and lower panels, w_{re} are taken as $w_{re} = -1/3, 0$ and 1 in each panel from left to right, the values of f/M_p and m are taken as the boundary values of the GNI model given by the data from P18+BK15 at 68% CL.

It can be seen that the high limit of the reheating temperature T_{re} and the limits of N_* can be obtained by the physical condition that the reheating e-folding number N_{re} should be non-negative. There are the maximum and minimum values of N_* for the cases of $w_{re} < 1/3$ and $w_{re} > 1/3$, respectively, i.e., $N_*^{max} = 56.34$ and $N_*^{min} = 55.5$. Moreover, the ranges of corresponding values of reheating parameters increase first and then decrease with the increasing w_{re} . And we can find that N_{re} and T_{re} are slightly more sensitive to the value of m than the value of f . When $w_{re} < 1/3$, N_{re} increases and T_{re} decreases at the fixed value of m (or f/M_p) with increasing f/M_p (or m). When $w_{re} > 1/3$, the reheating parameters evolve in the opposite trends. The concrete results

of the corresponding ranges of values of N_{re} and $\log_{10}(T_{re}/\text{GeV})$ for $w_{re} = -1/3, 0$ and 1 in the ranges of $\log_{10}(f/M_p) = 0.62^{+0.17}_{-0.18}$ and $m = 0.35^{+0.13}_{-0.23}$ are listed in Table 1.

Table 1. The corresponding ranges of values of N_{re} and $\log_{10}(T_{re}/\text{GeV})$ for $w_{re} = -1/3, 0$ and 1 in the ranges of $\log_{10}(f/M_p) = 0.62^{+0.17}_{-0.18}$ and $m = 0.35^{+0.13}_{-0.23}$.

w_{re}	N_{re}	$\log_{10}(T_{re}/\text{GeV})$
$-1/3$	$0 - 12.7$	$12.6 - 15.3$
0	$0 - 25.5$	$7.0 - 15.3$
1	$0 - 9.0$	$9.5 - 15.3$

4.2. The two-phase reheating

Below we consider the reheating scenario as a simple case of two-phase process. After the end of inflation, scalar field inflaton starts to oscillate and decay into radiation field χ which is the so-called oscillation phase. At the equal scale, when the energy density of the oscillation field equals to the one of relativistic particle field, i.e., the expansion Hubble constant H equals to the decay rate Γ , the universe is going to be dominated by radiation. Therefore, $H = \Gamma$ is regarded as the sign of completing the simplest two-phase reheating. Note that, the system is not at thermal equilibrium during the process, and it has gone through a process called thermalization phase. When the ϕ field oscillates around its minimum value, the potential Eq. (13) has an approximate form of $V(\phi) \propto \phi^{2m}$. For the ϕ^{2m} form-like potential, the EoS can be expressed as [36, 43]:

$$w_{sc} = \frac{m-1}{m+1}. \quad (30)$$

The reheating e-folding number N_{re} is reconsidered as the sum of two phases, N_{sc} and N_{th} . We know that $N_{sc} = \ln \frac{a_{eq}}{a_{end}}$ and $N_{th} = \ln \frac{a_{re}}{a_{eq}}$, where a_{eq} is the dividing point of the two phases. They can be written as

$$N_{sc} = -\frac{1}{3(1+w_{sc})} \ln \frac{\rho_{eq}}{\rho_{end}}, \quad (31)$$

and

$$N_{th} = -\frac{1}{4} \ln \frac{\rho_{re}}{\rho_{eq}}, \quad (32)$$

where $w_{th} = w_r = 1/3$ has been adopted in Eq. (32).

Based on the continuity equation, ρ_{eq} can be expressed as

$$\rho_{eq} = \frac{3}{2} V_{end} \exp[-3(1+w_{sc})N_{sc}]. \quad (33)$$

Finally, Eqs. (31) and (32) can be rewritten as follows:

$$N_{sc} = \frac{4}{1-3w_{sc}} \left[-N_* - \frac{1}{3} \ln \frac{11g_{re}}{43} - \frac{1}{4} \ln \frac{45V_{end}}{g_{re}\pi^2} - \ln \frac{k_*}{T_\gamma} + \frac{1}{2} \ln \frac{\pi^2 M_{pl}^2 r A_s}{2} \right], \quad (34)$$

$$T_{re}e^{N_{th}} = \exp\left[-\frac{3}{4}(1+w_{sc})N_{sc}\right] \left(\frac{45V_{end}}{g_{re}\pi^2}\right)^{1/4}. \quad (35)$$

Figure 10 shows the evolutions of oscillation e-folding number N_{sc} and the temperature $T_{re}e^{N_{th}}/\text{GeV}$ with N_* . We find N_{sc} decreases, while $T_{re}e^{N_{th}}$ increases

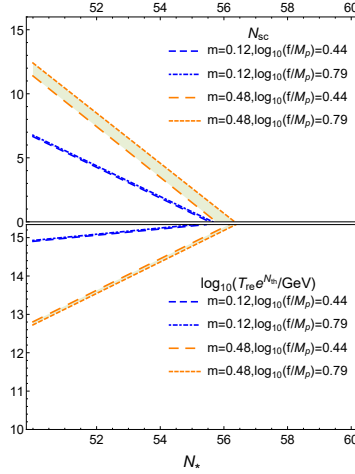


Figure 10. The evolutions of N_{sc} and $T_{re}e^{N_{th}}/\text{GeV}$ with respect to N_* in the two-phase reheating scenario are respectively plotted in the upper and lower panels, the values of f/M_p and m are taken as the boundary values of the GNI model given by the data from P18+BK15 at 68% CL.

with increasing N_* for the fixed values of f/M_p and m . Similar to the cases of general reheating phase, $N_{sc} \geq 0$ is required in order to make the two-phase reheating meaningful. The values of N_{sc} and $T_{re}e^{N_{th}}/\text{GeV}$ are in the ranges of $[0, 12.4]$ and $[12.7, 15.3]$, respectively.

In addition, we consider the elementary decay $\phi \rightarrow \chi\chi$ with the interaction $-g\phi\chi^2$, where g respectively the coupling constant. And following Ref. [36], we take the corresponding decay rate Γ as $\Gamma_{\phi \rightarrow \chi\chi} = \frac{g^2}{8\pi m_\phi}$, where m_ϕ is the mass of inflaton. Considering the Friedmann Equation $H^2 = \frac{\rho_{eq}}{3M_p^2}$ and the equality of $H = \Gamma$, it can be directly obtained that $(\frac{\rho_{eq}}{3M_p^2})^{1/2} = \frac{g^2}{8\pi m_\phi}$. Substituting Eqs. (30) and (33) into the above equation, the coupling constant g of the GNI model can be deduced as follows:

$$g = \sqrt{\frac{8\pi m_\phi}{M_p}} \left(\frac{V_{end}}{2}\right)^{1/4} \exp\left[-\frac{3m}{2(m+1)}N_{sc}\right]. \quad (36)$$

Utilizing $V_{end} \sim 2^{1-m}\Lambda^4(\frac{mM_p}{f})^{2m}$, the effective mass of inflaton $m_\phi^2 \sim m\frac{\Lambda^4}{f^2}$ at vacuum and Eq. (34), g can be expressed in terms of (N_*, f, m) . Therefore, we can give the evolution of the coupling constant g to realize a successful simplest two-phase reheating scenario.

In Figure 11, we plot the coupling constant g with respect to N_* , the solid (red) line corresponds to $N_* = 56.34$ from the requirement of $N_{sc} \geq 0$. From Figure 11, we

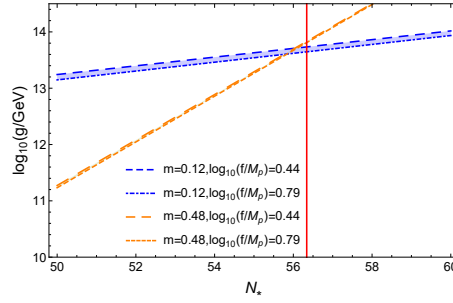


Figure 11. The evolution trajectories of the coupling constant g/GeV with respect to N_* , the values of f/M_p and m are taken as the boundary values of the GNI model given by the data from P18+BK15 at 68% CL.

find that the value of g increases with N_* for the fixed values of f/M_p and m . Besides, it shows that the value of g is more sensitive to the value of m than the value of f . And g decreases with increasing f for the fixed value of N_* and m . However, it decreases first and then increases with increasing m for the fixed value of N_* and f , there are turning points for $\log_{10}(f/M_p) = 0.79$ and 0.44 as $N_* = 55.8$ and 56.0 , respectively. The minimum value of g to complete the two-phase reheating is at the order of magnitude of 10^{11}GeV .

5. conclusions

In summary, in the paper we have in detail investigated the generalized natural inflationary (GNI) model according to the latest observational data from Planck 2018 plus BK15. As we discussed above, the constraints on the observables n_s and r for $\Lambda\text{CDM} + r$ model by means of the available Cosmomc code are given as $n_s = 0.9659 \pm 0.0044$ at 68%CL and $r < 0.0623$ at 95%CL (Planck TT,TE,EE+lowE+lensing+BK15).

For the GNI model, n_s and r have been expressed by N_* , f/M_p and m , thus the allowable parameter space of $(f/M_p, m)$ in the range of $N_* \in [50, 60]$ have been obtained as $\log_{10}(f/M_p) = 0.62^{+0.17}_{-0.18}$ and $m = 0.35^{+0.13}_{-0.23}$ at 68%CL. The general reheating parameters in the GNI model are the functions of N_* , f , m and w_{re} . Thus, we have obtained the evolutions of N_{re} and $\log_{10}(T_{re}/\text{GeV})$ with N_* for $w_{re} = -1/3, 0$ and 1 , respectively. The corresponding ranges of values have been shown as $N_{re} \leq 25.5$ and $7 \leq \log_{10}(T_{re}/\text{GeV}) \lesssim 15$ within the obtained allowable parameter space when $w_{re} = 0$. As for the two-phase reheating, the parameters are the functions of N_* , f and m , the values of N_{sc} and $T_{re}e^{N_{th}}/\text{GeV}$ are in the ranges of $[0, 12.4]$ and $[12.7, 15.3]$, and the values of the coupling constant g/GeV is in the range of $11.2 \leq \log_{10}(g/\text{GeV}) \leq 13.8$ within the allowable parameter space. It follows that the parameter m has the significant effect on the behaviors of the GNI model.

Acknowledgments

We thank Dr. Xue Zhang for her helpful discussion on the Monte Carlo method. This work is supported by the National Natural Science Foundation of China (Grant Nos. 11575075, 11705079 and 11865012).

References

- [1] A.H. Guth, “The inflationary universe: A possible solution to the horizon and flatness problems,” *Phys. Rev. D* 23, 347-356 (1981).
- [2] A.D. Linde, “A new inflationary universe scenario: A possible solution of the horizon, flatness, homogeneity, isotropy and primordial monopole problems,” *Phys. Lett. B* 108, 389-393 (1982).
- [3] A. Albrecht, P.J. Steinhardt, “Cosmology for grand unified theories with radiatively induced symmetry breaking,” *Phys. Rev. Lett.* 48, 1220-1223 (1982).
- [4] S. W. Hawking, I. G. Moss, “Supercooled phase transitions in the very early universe,” *Phys. Lett. B* 110, 35-38 (1982).
- [5] A. D. Linde, “Chaotic inflation, *Phys. Lett. B* 129, 177-181 (1983).
- [6] V. F. Mukhanov, G. Chibisov, “Quantum fluctuation and nonsingular universe,” *JETP Lett.* 33, 532-535 (1981).
- [7] S. W. Hawking, “The Development of Irregularities in a Single Bubble Inflationary Universe,” *Phys. Lett. B* 115, 295-297 (1982).
- [8] A. H. Guth, S. Y. Pi, “Fluctuations in the new inflationary universe, *Phys. Rev. Lett.* 49, 1110-1113 (1982).
- [9] Starobinsky, Alexei A., “A New Type of Isotropic Cosmological Models Without Singularity”, *Phys. Lett. B* 91, 99-102 (1980).
- [10] L. Boubekeur, D. H. Lyth, “Hilltop inflation,” *JCAP* 0507, 010 (2005).
- [11] K. Freese, J. A. Frieman, A. V. Olinto, “Natural Inflation with Pseudo Nambu-Goldstone Bosons,” *Phys. Rev. Lett.* 65, 3233 (1990).
- [12] F. C. Adams, J. R. Bond, K. Freese, et al., “Natural inflation: Particle physics models, power-law spectra for large-scale structure, and constraints from Cosmic Background Explorer,” *Phys. Rev. D* 47, 427 (1993).
- [13] R. Kallosh, A. Linde, “Superconformal generalizations of the Starobinsky model,” *JCAP*, 1306, 028 (2013).
- [14] R. Kallosh, A. Linde, D. Roest, “Superconformal Inflationary α -Attractors,” *JHEP*, 1311, 198 (2013).
- [15] A. R. Liddle, D. H. Lyth, “COBE, gravitational waves, inflation and extended inflation,” *Phys. Lett. B* 291, 391-398 (1992).
- [16] A. R. Liddle, P. Parsons, and J. D. Barrow, “Formalizing the slow-roll approximation in inflation,” *Phys. Rev. D* 50, 7222-7232 (1994).
- [17] P. J. Steinhardt, M. S. Turner, “A Prescription for Successful New Inflation,” *Phys. Rev. D* 29, 2162-2171 (1984).
- [18] J. B. Munoz, M. Kamionkowski, “Equation-of-state parameter for reheating,” *Phys. Rev. D* 91, 043521 (2015).
- [19] R-G. Cai, Z-K. Guo, S-J. Wang, “Reheating phase diagram for single-field slow-roll inflationary models,” *Phys. Rev. D* 92, 063506 (2015).
- [20] Q-G Huang, K Wang, and S Wang, “Inflation model constraints from data released in 2015,” *Phys. Rev. D* 93, 103516 (2016).
- [21] J. Martin, C. Ringeval, V. Vennina, “Encyclopædia Inflationaries,” *Phys. Dark Univ.* 5 -6, 75 (2014).

- [22] P. A. R. Ade, et al.(Planck Collaboration), “Planck 2013 results. XVI. Cosmological parameters,” *Astronomy. Astrophysics*, 571, A16 (2014).
- [23] P. A. R. Ade, et al.(Planck Collaboration), “Planck 2013 results. XXII. Constraints on inflation,” *Astronomy. Astrophysics*, 571, A22 (2014).
- [24] P. A. R. Ade, et al.(Planck Collaboration), “Planck 2015 results. XIII. Cosmological parameters,” *Astronomy. Astrophysics*, 594, A13 (2016).
- [25] P. A. R. Ade, et al.(Planck Collaboration), “Planck 2015 results. XX. Constraints on inflation,” *Astronomy. Astrophysics*, 594, A20 (2016).
- [26] N. Aghanim, et al.(Planck Collaboration), “Planck 2018 results. VI. Cosmological parameters,” arXiv:1807.06209.
- [27] Y. Akrami, et al.(Planck Collaboration), “Planck 2018 results. X. Constraints on inflation,” arXiv:1807.06211.
- [28] P. A. R. Ade, et al.(Keck Array and BICEP2 Collaborations), “Improved Constraints on Cosmology and Foregrounds from BICEP2 and Keck Array Cosmic Microwave Background Data with Inclusion of 95 GHz Band,” *Phys. Rev. Lett.* 116, 031302 (2016).
- [29] D. I. Podolsky, G. N. Felder, L. Kofman, and M. Peloso, “Equation of state and beginning of thermalization after preheating,” *Phys. Rev. D* 73, 023501 (2006).
- [30] P. A. R. Ade, et al.(Keck Array and BICEP2 Collaborations), “Constraints on Primordial Gravitational Waves Using Planck, WMAP, and New BICEP2/Keck Observations through the 2015 Season,” *Phys. Rev. Lett.* 121, 221301 (2018).
- [31] L. F. Abbott, E. Farhi, M. B. Wise, “Particle production in the new inflationary cosmology,” *Phys. Lett. B* 117, 28 (1982).
- [32] L. Kofman, A. D. Linde, A. A. Starobinsky, “Towards the theory of reheating after inflation,” *Phys. Rev. D* 56, 3258-3295 (1997).
- [33] R. Allahverdi, R. Brandenberger, F.Y. Cyr-Racine, et.al., “Reheating in inflationary cosmology: Theory and applications,” *Annu. Rev. Nucl. Part. Sci.*, 60, 27 (2010).
- [34] A. Lewis, and S. Bridle, “Cosmological parameters from CMB and other data: A Monte Carlo approach,” *Phys. Rev. D* 66, 103511 (2002).
- [35] M. Drewes, “What can the CMB tell about the microphysics of cosmic reheating?”, *JCAP*03, 013 (2016).
- [36] Y. Ueno, K. Yamamoto, “Constraints on α -attractor inflation and reheating,” *Phys. Rev. D* 93, 083524 (2016).
- [37] C. Cheng, Q. G. Huang and W. Zhao, “Constraints on the extensions to the base Λ CDM model from BICEP2, Planck and WMAP,” *Sci. China Phys. Mech. Astron.* 57, 1460. (2014).
- [38] Q. G. Huang, S. Wang and W. Zhao, “Forecasting sensitivity on tilt of power spectrum of primordial gravitational waves after Planck satellite,” *JCAP* 1510, 035 (2015).
- [39] D. H. Lyth, “What would we learn by detecting a gravitational wave signal in the cosmic microwave background anisotropy?,” *Phys. Rev. Lett.* 78, 1861 (1997).
- [40] J. Martin, C. Ringeval, “First CMB constraints on the inflationary reheating temperature,” *Phys. Rev. D* 82, 023511 (2010).
- [41] L. Dai, M. Kamionkowski, J. Wang, “Reheating Constraints to Inflationary Models,” *Phys. Rev. Lett.* 113, 041302 (2014).
- [42] S. Dodelson., “Modern Cosmology” (Amsterdam, Boston: Academic Press, 2003).
- [43] V. F. Mukhanov, “Physical Foundations of Cosmology” (Cambridge Universe Press, Cambridge, England, 2005).